

## Theory of high-field transport of holes in GaAs and InP

Kevin Brennan and Karl Hess

Department of Electrical Engineering and Coordinated Science Laboratory, University of Illinois at Urbana—Champaign, Urbana, Illinois 61801

(Received 6 February 1984)

Calculations of the steady-state drift velocity and impact ionization rate of holes in the valence bands of GaAs and InP are presented based on a Monte Carlo simulation with the unique inclusion of a complete band structure (derived using the  $\vec{k}\cdot\vec{p}$  method) and quantum effects such as collision broadening. The results are found to fit the experimental data well throughout an enormous range of applied electric fields. No appreciable anisotropy in the impact ionization rate is obtained theoretically in either material. The impact ionization rate in InP is much lower than in GaAs largely because of the greater density of states in InP and the corresponding higher hole-phonon scattering rate. A possible explanation of the difference in the ratio of electron over hole ionization rates in GaAs and InP is also presented.

### I. INTRODUCTION

High-field transport is of prime importance in many devices<sup>1</sup> such as Gunn diodes, field-effect transistors, and other devices,<sup>2-4</sup> as their physical dimensions shrink in size. Phenomena such as impact ionization can occur and greatly effect device performance. In some devices, particularly avalanche photodiodes, carrier multiplication through impact ionization is essential to their operation. The performance of these devices depends sensitively on

the electron and hole ionization coefficients and their ratio.<sup>5-10</sup> It is therefore desirable to understand the basic high-field mechanisms in great detail.

A charge carrier must have an energy at least as large as the band gap in order to impact-ionize because of energy conservation. Therefore in semiconductors such as GaAs and InP with relatively large band gaps, the carriers must be at high energies in the band before they can impact-ionize. In the past, most theoretical studies<sup>11-15</sup> of impact ionization have been based upon phenomenological fits which contain several adjustable parameters whose physical significance is not well understood. The most widely used of these theories is that given by Baraff,<sup>13</sup> but the parameters employed in Baraff's theory

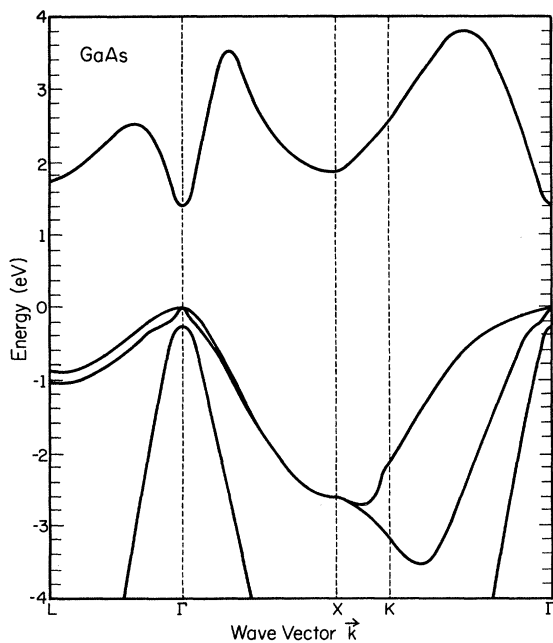


FIG. 1.  $E(k)$  relation for GaAs including the first conduction band and the heavy-hole, light-hole, and split-off valence bands. The conduction band is sketched based on the pseudopotential calculation of Cohen and Bergstresser (Ref. 24), while the valence bands are based on a  $\vec{k}\cdot\vec{p}$  calculation (Ref. 22).

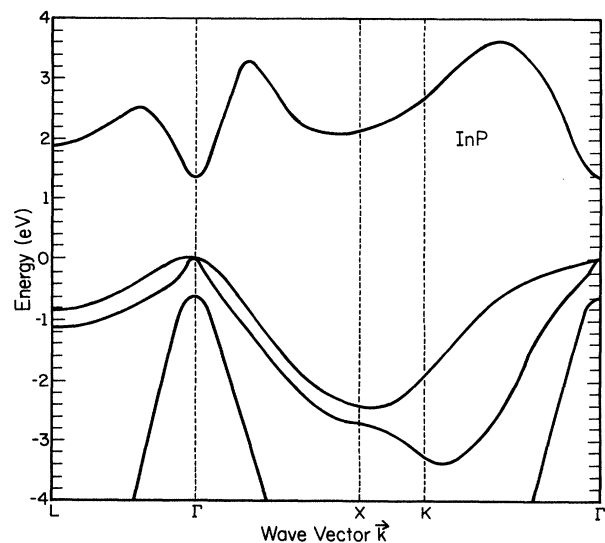


FIG. 2.  $E(k)$  relation for InP including the first conduction band and the heavy-hole, light-hole, and split-off valence bands. The conduction band is sketched based on the pseudopotential calculation of Cohen and Bergstresser (Ref. 24), while the valence bands are based on a  $\vec{k}\cdot\vec{p}$  calculation (Ref. 22).

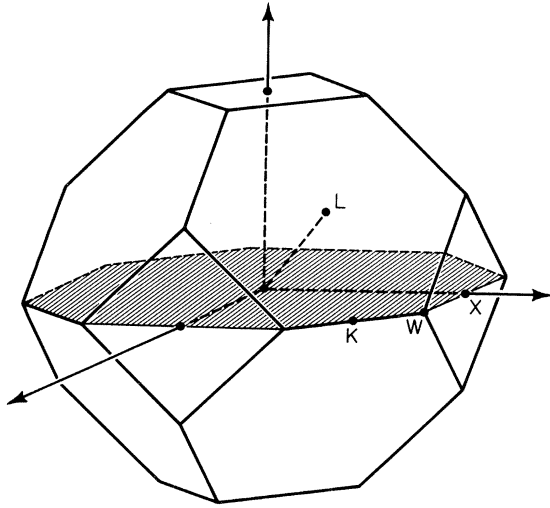
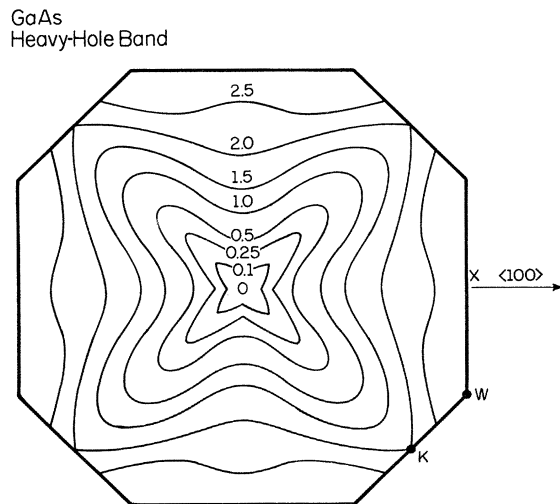
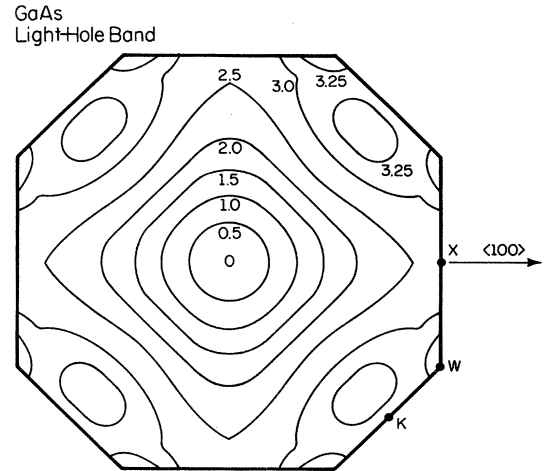


FIG. 3. Cross section of the Brillouin zone.

are difficult if not impossible to understand from first principles. The recent work of Shichijo and Hess<sup>16</sup> has provided a complete theory of impact ionization which can calculate the impact-ionization parameters from rather elementary principles. The success of their theory is due to the abandonment of the effective-mass approximation, which totally breaks down at high energies, in favor of a complete band structure calculated using the pseudo-potential method.

A similar theory for holes has not been given before and it has not been demonstrated from first principles why the ratio of electron,  $\alpha$ , over hole,  $\beta$ , ionization coefficients is reversed between GaAs and InP. The recent work of Ridley<sup>17,18</sup> suggests that the ratio of  $\alpha$  over  $\beta$  can be entirely determined by the ratio of ionization threshold energies. However, his results show that the ratio of  $\alpha$  over  $\beta$  is less than 1 for both GaAs and InP over a wide range of applied fields, in direct contradiction to recent experimental results.<sup>19-21</sup>

FIG. 4. Isoenergy lines of the heavy-hole band of GaAs in the cross section shown in Fig. 3. The numbers represent the energies measured from the  $\Gamma$  minimum in eV.FIG. 5. Isoenergy lines of the light-hole band of GaAs in the cross section shown in Fig. 3. The numbers represent the energies measured from the  $\Gamma$  minimum in eV.

In this paper, we present calculations of the hole impact-ionization rate and steady-state drift velocity in GaAs and InP using a Monte Carlo calculation<sup>16</sup> including a realistic band structure based on a  $\vec{k}\cdot\vec{p}$  calculation.<sup>22</sup> Using the results obtained here and results for electrons presented elsewhere,<sup>23</sup> we demonstrate how the reversal of the ratio of the electron and hole ionization coefficients in GaAs and InP can be understood. Along with the work of Shichijo and Hess,<sup>16</sup> this paper presents a step towards the complete understanding of both electron and hole impact ionization.

## II. BAND STRUCTURE

The valence-band structure is calculated using the  $\vec{k}\cdot\vec{p}$  method of Kane.<sup>22</sup> The effect of the spin-orbit interaction, which forms the split-off band, is included in Kane's calculation. It is essential to include the effects of the split-off band in hole-transport calculations because of its influence upon the other bands, particularly the light-hole

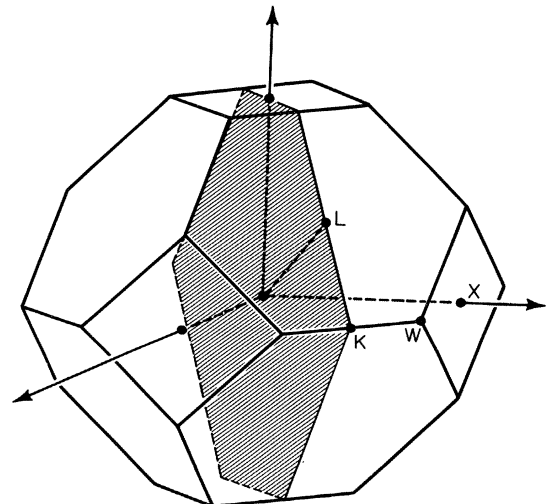


FIG. 6. Cross section of the Brillouin zone.

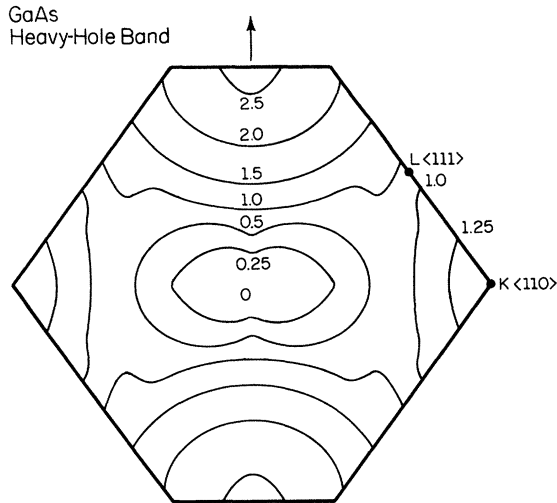


FIG. 7. Isoenergy lines of the heavy-hole band of GaAs in the cross section shown in Fig. 6. The numbers represent the energies measured from the  $\Gamma$  minimum in eV.

band. The split-off band “repels” the other bands in such a way that they do not cross. If the split-off band is not included in the calculation, the light-hole band appears to be rather parabolic and isotropic.<sup>24</sup> As can be seen from Figs. 1 and 2, it is clear that when the split-off band is included, the light-hole band is strongly warped and follows

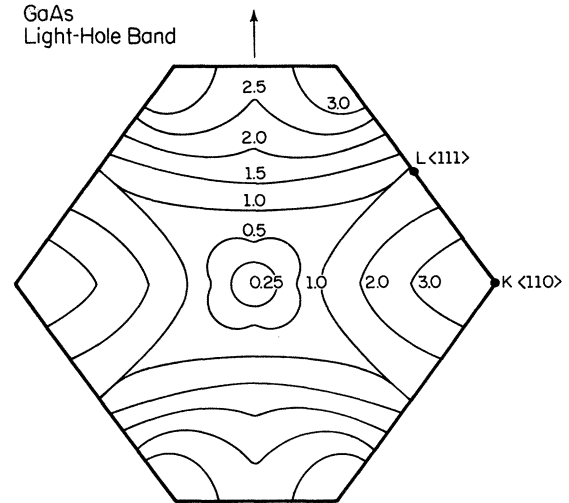


FIG. 8. Isoenergy lines of the light-hole band of GaAs in the cross section shown in Fig. 6. The numbers represent the energies measured from the  $\Gamma$  minimum in eV.

the heavy-hole band quite closely at high energy. This reemphasizes that the effective-mass approximation is an unrealistic description of the light- and heavy-hole bands.

Aside from its effect upon the other valence bands, the split-off band is of direct importance in hole transport. Owing to the small mass in the split-off band, holes

TABLE I. Parameters for GaAs hole-transport program.

Bulk material parameters <sup>a</sup>	
Lattice constant (Å)	5.65
Density (g/cm <sup>3</sup> )	5.36
Energy-band gap ( $T=300$ K) (eV)	1.424
Dielectric constants: $\epsilon_{\infty}$	10.92
$\epsilon_0$	12.9
Crystal elastic constants (dyn/cm <sup>2</sup> ): $C_{11}$	$11.88 \times 10^{11}$
$C_{12}$	$5.38 \times 10^{11}$
$C_{44}$	$5.49 \times 10^{11}$
[100] longitudinal sound velocity $S_l$ (cm/sec)	$4.73 \times 10^5$
[100] transverse sound velocity $S_t$ (cm/sec)	$3.34 \times 10^5$
Scattering-rate parameters <sup>b</sup>	
Effective masses: heavy-hole band $m_{HH}$	$0.45 m_0$
light-hole band $m_{LH}$	$0.082 m_0$
split-off band $m_{SO}$	$0.154 m_0$
Optical-phonon energy (eV)	0.035
Deformation-potential constants (eV): $a$	3.1
$b$	1.7
$d$	4.4
Impact-ionization—rate parameters	
Set 1: <sup>c</sup> Threshold energy $E_{th}$ (eV)	1.70
Multiplicative factor $p$	0.25
Set 2: Bands 1 and 2: $E_{th}$ (eV)	1.80
$p$	0.25
Band 3: $E_{th}$ (eV)	1.424
$p$	0.25

<sup>a</sup>Reference 43.

<sup>b</sup>References 43 and 32.

<sup>c</sup>Values of  $E_{th}$  and  $p$  are identical for all three bands.

TABLE II. Parameters for InP hole-transport program.

Bulk material parameters <sup>a</sup>	
Lattice constant (Å)	5.868
Density (g/cm <sup>3</sup> )	4.787
Energy-band gap ( $T=300$ K) (eV)	1.35
Dielectric constants: $\epsilon_\infty$	9.52
$\epsilon_0$	12.35
Crystal elastic constants (dyn/cm <sup>2</sup> ): $C_{11}$	$10.22 \times 10^{11}$
$C_{12}$	$5.76 \times 10^{11}$
$C_{44}$	$4.60 \times 10^{11}$
[100] longitudinal sound velocity $S_l$ (cm/sec)	$5.13 \times 10^5$
[100] transverse sound velocity $S_t$ (cm/sec)	$3.10 \times 10^5$
Scattering-rate parameters <sup>b</sup>	
Effective masses: heavy-hole band $m_{HH}$	$0.45 m_0$
light-hole band $m_{LH}$	$0.12 m_0$
split-off band $m_{SO}$	$0.21 m_0$
Optical-phonon energy (eV)	0.043
Deformation-potential constants (eV): $a$	2.8
$b$	1.55
$d$	4.4
Impact-ionization—rate parameters <sup>c</sup>	
Threshold energy $E_{th}$ (eV)	1.55
Multiplicative factor $p$	20.0

<sup>a</sup>Reference 44.

<sup>b</sup>References 44 and 32.

<sup>c</sup>Values of  $E_{th}$  and  $p$  are identical for all three bands.

within it can be accelerated to high energies by an applied electric field. At the  $\Gamma$  point the split-off band is nondegenerate with the heavy- and light-hole bands. The energy difference between the bands is known as the split-off energy. When the split-off energy is large, much greater than  $kT$ , the split-off band is virtually unoccupied at zero applied electric field. The holes must be scattered to the split-off band from either the heavy- or light-hole bands by either deformation-potential or polar-optical scattering. Of course, by energy conservation, a hole must drift to an energy close to or above the split-off energy before it can be scattered to the split-off band. As we shall see, the

magnitude of the split-off energy can greatly effect the importance of the split-off band in impact ionization.

To further illustrate the nature of the valence bands, particularly the heavy- and light-hole bands, at high energy, cross-sectional cuts through the Brillouin zone are presented in Figs. 3–8 for GaAs. As can be readily seen from these figures, the heavy- and light-hole bands deviate strongly from parabolic behavior and show a very complicated structure away from the  $\Gamma$  point. Even at very low energy,  $<20$  meV, the bands are greatly distorted.<sup>25</sup> Nonparabolic behavior of the bands is as strong in InP. Comparable drawings of isoenergy lines in different

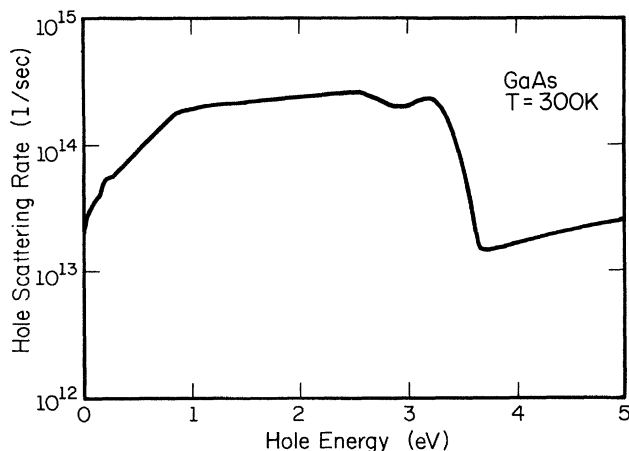


FIG. 9. Phonon scattering rate in GaAs as a function of hole energy. The rate is calculated using a field-theoretic scheme and the impact-ionization rate is omitted.

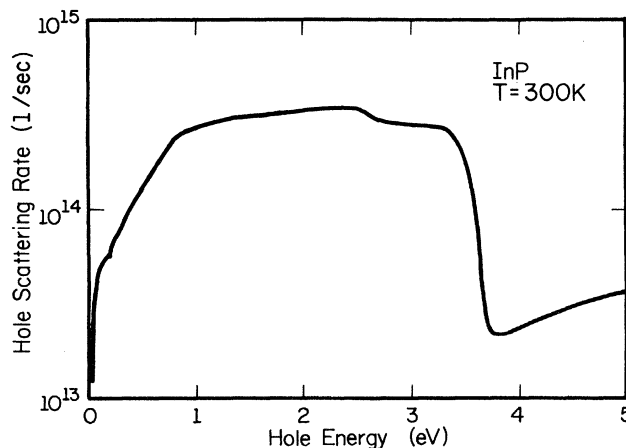


FIG. 10. Phonon scattering rate in InP as a function of hole energy. The rate is calculated using a field-theoretic scheme and the impact-ionization rate is omitted.

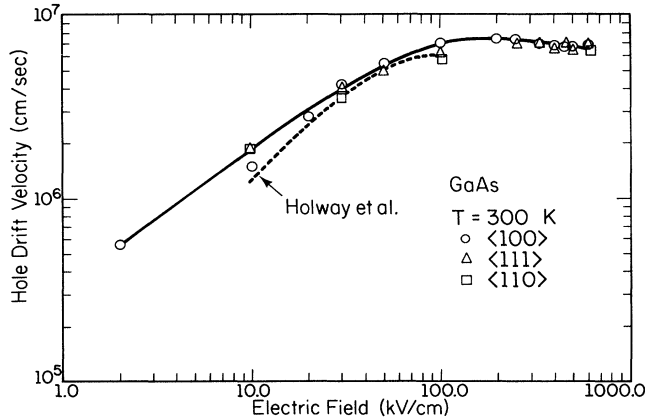


FIG. 11. Calculated steady-state drift velocity in GaAs at room temperature compared with the experimental data of Holway *et al.* (Ref. 34). The experimental data are marked with a dashed line. The solid line is meant as a guide for the eye to show the trend in the calculated data.

Brillouin-zone cuts in InP show a strong resemblance to those for GaAs. They have been omitted here for brevity. Figures 3–8 clearly illustrate that any complete theory of high-energy transport must take into account the full nature of the band structure.

### III. PHONON SCATTERING RATE

In the valence band the predominant scattering mechanisms are polar-optical and deformation-potential scattering—when the effects of impurities can be ignored.<sup>26,27</sup> For simplicity, we neglect impurity scattering in our calculations. The total scattering rate includes both intraband and interband scattering and is based on the total density of states of all three valence bands using a field-theoretic approach.<sup>23,28,29</sup> The individual phonon scattering mechanisms are calculated using the approach of Costato and Reggiani.<sup>26,27,30</sup> The principal scattering agents are acoustic, nonpolar, and polar-optical phonons.

The acoustic-phonon scattering rate is calculated using the method of Canali *et al.*<sup>30</sup> In their calculation, instead of the usual equipartition approximation, the Bose-Einstein distribution function is expanded in a power series and integrated to obtain the approximate total scattering rate. This is necessary since at high energy, the

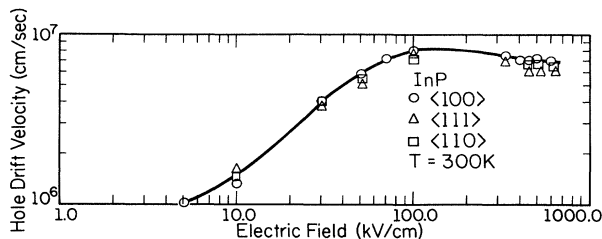


FIG. 12. Calculated steady-state drift velocity in InP at room temperature. Experimental data are not presently available. The solid line is meant as a guide for the eye to show the trend in the calculated data.

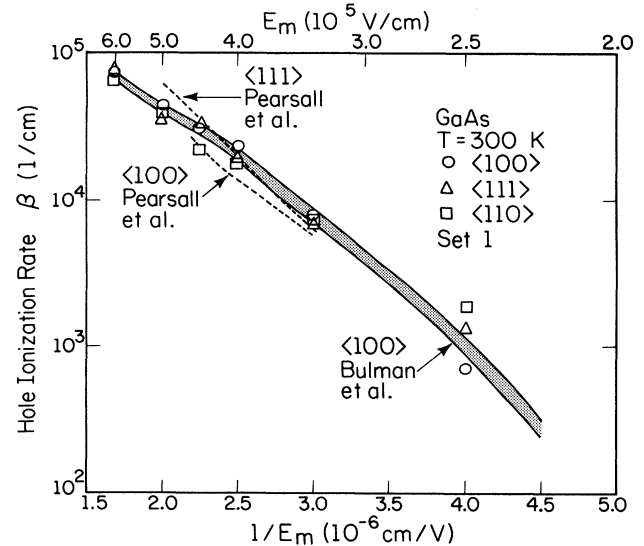


FIG. 13. Calculated hole impact-ionization rate in GaAs as a function of inverse field in three crystallographic directions. The shaded region indicates the range of available experimental data (Ref. 19). All the calculations are made using set-1 parameters.

energy lost or gained in an acoustic scattering event is not negligible, which makes the equipartition approximation questionable.<sup>29</sup> The acoustic-phonon coupling constant  $E_1^2$  is given by<sup>26</sup>

$$E_1^2 = \left[ \frac{1}{3} + \frac{2}{3} (S_l/S_t)^2 \right] \left[ a^2 + (C_l/C_t) (b^2 + \frac{1}{2} d^2) \right], \quad (1)$$

where  $S_l$  is the longitudinal sound velocity and  $S_t$  is the transverse sound velocity. The values of  $C_l$  and  $C_t$  are given as

$$C_l = \frac{1}{5} (3C_{11} + 2C_{12} + 4C_{44}), \quad (2)$$

$$C_t = \frac{1}{5} (C_{11} - C_{12} + 3C_{44}),$$

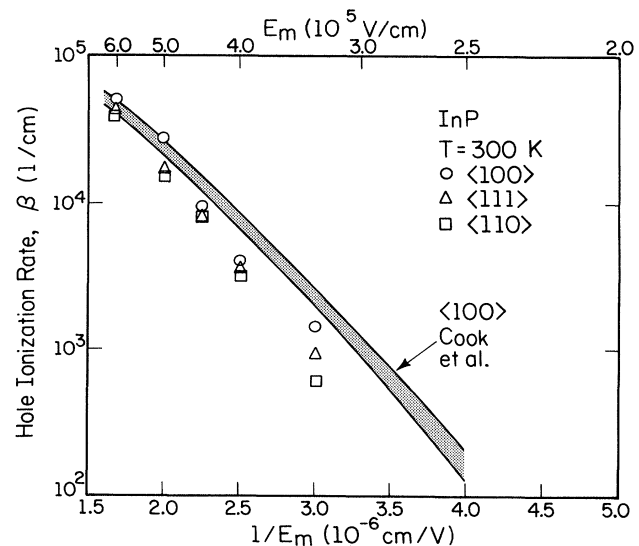


FIG. 14. Calculated hole impact-ionization rate in InP as a function of inverse field in three crystallographic directions. The shaded region indicates the range of available experimental data (Refs. 20 and 21).

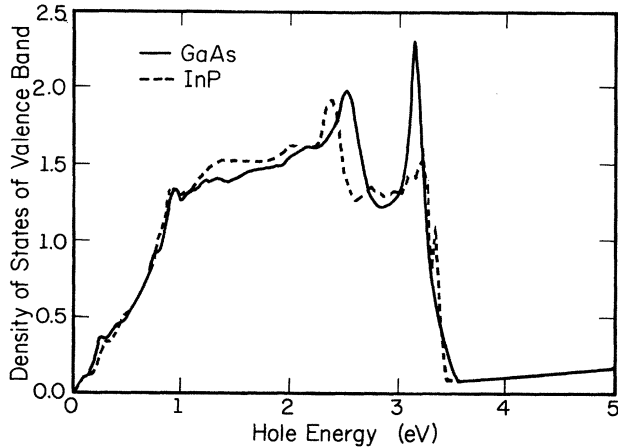


FIG. 15. Total density of states of the heavy-hole, light-hole, and split-off bands of GaAs and InP as a function of hole energy.

where  $C_{11}$ ,  $C_{12}$ , and  $C_{44}$  are the crystal elastic constants. All of the parameters used in the calculations are collected in Tables I and II for GaAs and InP, respectively.

The transition probabilities due to nonpolar-optical scattering can be written in a form analogous to that for acoustic-phonon scattering<sup>31</sup> containing the optical deformation-potential constant  $d_0$ . However,  $d_0$  cannot be directly determined from piezoresistance data.<sup>26</sup> It is useful then to formulate the nonpolar-optical scattering rate in terms of a more easily determined quantity. The optical-phonon coupling constant  $(DK)^2$  can be determined from the acoustic deformation-potential constant as<sup>32</sup>

$$(DK)^2 = 4 \left( \frac{\omega_0}{S_l} \right)^2 E_1^2, \quad (3)$$

where  $\omega_0$  is the optical phonon frequency.

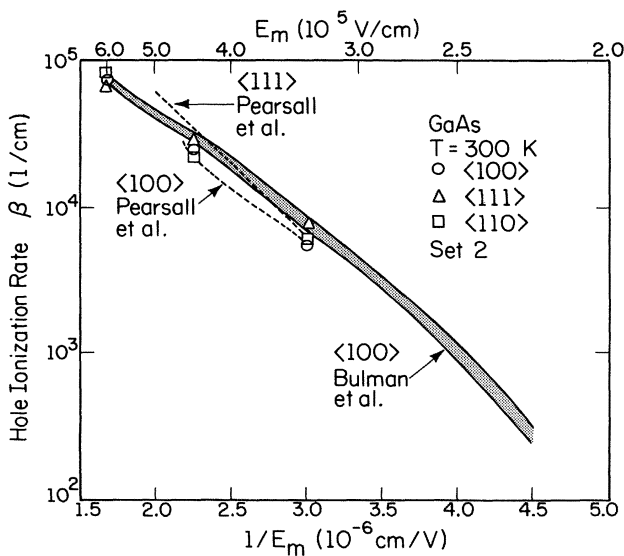


FIG. 16. Calculated hole impact-ionization rate in GaAs as a function of inverse field in three crystallographic directions. The shaded region indicates the range of available experimental data (Ref. 19). The data of Pearsall *et al.* are from Ref. 45. All the calculations are made using set-2 parameters.

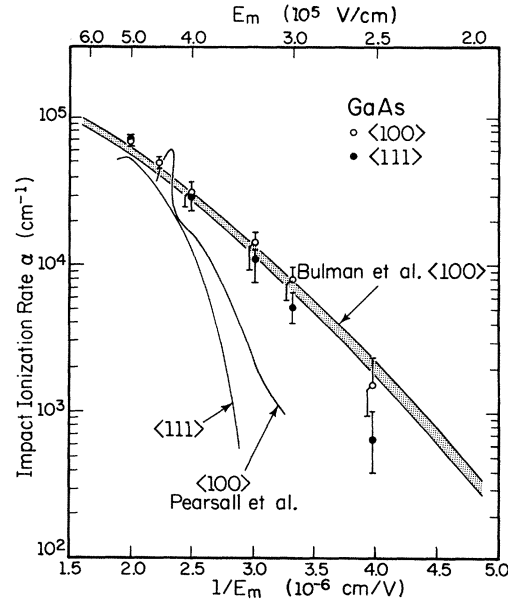


FIG. 17. Calculated electron impact-ionization rate as a function of inverse electric field along with experimental measurements (Ref. 19) in the  $\langle 100 \rangle$  direction in GaAs. The data of Pearsall *et al.* are from Ref. 45.

The results of Costato and Reggiani<sup>27</sup> show that the overlap corrections due to the mixing of Bloch states introduce significant corrections to the overall hole-polar-optical-phonon scattering rate. We have included these effects into our calculation. The parameters used in the calculation of the polar-optical scattering rate are also collected in Tables I and II.

The total hole-phonon scattering rate is calculated for both GaAs and InP using a field-theoretic approach at hole energies above 0.5 eV which is fitted to the low-energy scattering rate calculated by using the method of

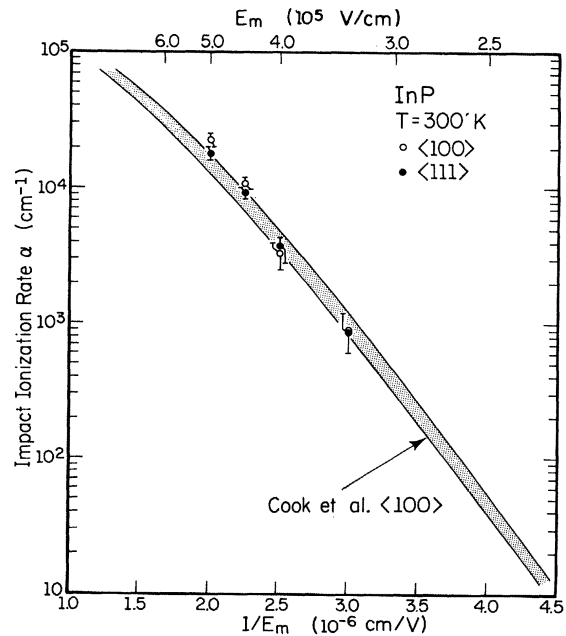


FIG. 18. Calculated electron impact-ionization rate as a function of inverse electric field along with experimental measurements (Ref. 20) in the  $\langle 100 \rangle$  direction in InP.

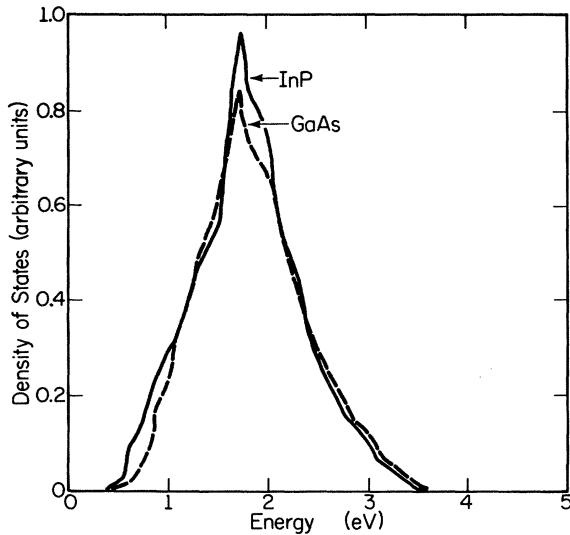


FIG. 19. Total density of states of the first conduction bands of GaAs and InP as a function of electron energy.

Costato and Reggiani.<sup>26,27</sup> The scattering rates are presented in Figs. 9 and 10. They include only the hole-phonon processes and do not include impact ionization. The relative strength of each scattering mechanism as a function of energy is calculated in the entire energy range from the results of Costato and Reggiani.<sup>26,27,30</sup> The results of this calculation are used to determine which scattering mechanism is active after it has been determined, from the total scattering rate, that a real event has occurred.

Impact ionization is treated as a separate scattering mechanism in accordance with the Keldysh theory.<sup>14</sup> There exist two adjustable parameters,  $E_{th}$  and  $p$ , in the Keldysh theory.  $E_{th}$  is the impact ionization threshold energy, while  $p$  is a numerical multiplicative factor which varies for each material. These parameters are chosen to fit the calculated impact ionization rate to the experimental results. The work of Tang<sup>29</sup> has demonstrated that previous theories for impact ionization using Keldysh's formalism with  $p \gg 1$  are incorrect since the high-energy tail of the energy distribution function is overly suppressed. By restricting  $p$  to low values,  $\sim 10.0$  or less, the range of acceptable values for the impact-ionization threshold is greatly limited particularly if only one band is considered in the calculation. Recent work on silicon<sup>33</sup> has shown that more than one set of parameters exists for the Keldysh formula if multiple bands are considered. This is because it cannot be determined *a priori* which band, if either, plays the dominant role in impact ionization. It is desirable to remove the parametrizations of the Keldysh theory, but this can only be done by reformulating the impact-ionization probability using a more exact inverse Auger calculation. It is important to notice that the parameters,  $p$ , and to some extent,  $E_{th}$  (which have to be chosen to fit the experiments), depend sensitively on the magnitude of the phonon scattering rates. Small uncertainties in the phonon scattering rate have a pronounced influence on  $p$  and (to a lesser extent)  $E_{th}$ . Our future work will attempt to address this problem.

#### IV. STEADY-STATE DRIFT-VELOCITY THEORY

Little experimental data exist on the hole drift velocity in compound semiconductors, and, to the authors' knowledge, none are available for holes in InP. Figure 11 shows both experimental<sup>34</sup> and calculated drift-velocity data for holes in GaAs. The experimental measurements are made for applied electric fields along only the  $\langle 100 \rangle$  direction, while the Monte Carlo calculations are made for fields oriented along the  $\langle 100 \rangle$ ,  $\langle 110 \rangle$ , and  $\langle 111 \rangle$  directions. As seen from Fig. 11, there is no significant anisotropy in the hole drift velocity through a large range of applied electric fields. The calculated results for the hole drift velocity in GaAs fit the experimental data extremely well.

The hole drift velocity is somewhat higher in InP (as seen in Fig. 12) than in GaAs, despite a greater scattering rate present in InP. The difference is only of the order of 10%, which is roughly the error in the calculation. Therefore, it is difficult to determine whether the drift-velocity difference is due to the different band structures or whether it is a statistical error. However, a similar situation occurs in the conduction bands of GaAs and InP. The work of Windhorn *et al.*<sup>35,36</sup> demonstrates that the electron drift velocity is higher in InP than in GaAs at high applied fields. Analysis of the saturation velocity of electrons in GaAs shows that it is approximately the same,  $7.0 \times 10^6$  cm/sec,<sup>37</sup> as that for holes,  $6.5 \times 10^6$  cm/sec. The saturation velocity for electrons,  $7.5 \times 10^6$  cm/sec, is also roughly the same as that for holes in InP,  $7.0 \times 10^6$  cm/sec, although both are larger than their counterparts in GaAs. It is most interesting that the saturation velocity of both electrons and holes in each material is essentially the same. Further experimental work is necessary to decide if the hole drift velocity is greater in InP than in GaAs, as is the case for the electrons.

#### V. IMPACT IONIZATION

As mentioned above, a hole must attain an energy at least as great as the energy-band gap in order to impact-ionize. Since both momentum and energy must be conserved during an impact-ionization event, the threshold energy for impact ionization is often significantly greater than the band gap.<sup>38</sup> In GaAs and InP all three valence bands—the heavy hole, light hole, and split-off—extend to energies far beyond the band gap at which impact ionization can occur. Owing to the strongly anisotropic behavior of the bands at high energy, a rigorous calculation of the threshold energy in all directions is difficult. It is common practice, then, to assume an isotropic threshold energy. Several quantum effects support the assumption of an isotropic threshold energy. Among these effects are electron-phonon—collision broadening, Stark-ladder effects, and intracollisional field effects. An isotropic threshold energy is also consistent with the theory of Kane.<sup>39</sup> If the isotropic threshold energy is sufficiently high, *threshold cannot be reached in certain directions*.<sup>40</sup> Therefore, the assumption of an isotropic ionization threshold energy does not preclude an anisotropic impact-ionization rate.

We have found that the Monte Carlo impact-

ionization—rate calculations can be fit to the experimental results in a variety of ways. As mentioned previously, there are two adjustable parameters,  $p$  and  $E_{th}$ , in the Monte Carlo calculations. In the first set of parameters we assume that the impact ionization behaves the same in all three bands; both  $p$  and  $E_{th}$  are identical in each of the bands. For the case of GaAs, the experimental results are fit extremely well through a wide range of applied fields, as seen in Fig. 13, by using a universal threshold of 1.70 eV, the effective threshold is still higher, and a universal  $p$  factor of 0.25. Calculations are made for applied fields along the  $\langle 100 \rangle$ ,  $\langle 110 \rangle$ , and  $\langle 111 \rangle$  directions. The results show that there is no anisotropy in the impact-ionization rate at high applied fields in GaAs. As the field decreases, there is more of a spread in the data. This may be due to statistical uncertainty since far fewer ionization events occur at low applied fields. A slight anisotropy in the impact-ionization rate at low applied fields is expected, however, because the “lucky” holes should contribute more to the impact-ionization rate. At low applied fields the hole distribution is centered closer to  $\vec{k} = \vec{0}$  than at high fields. Since the distribution is cooler, those holes which reach the ionization threshold do so only after gaining much energy from the field. Maximum energy will be gained from the field provided that the holes are not scattered much from the field direction. A small anisotropy in the ionization rate is then possible because a hole, due to the anisotropy of the band structure, will gain different amounts of energy along different field directions per drift. Consequently, a hole can reach the ionization threshold energy faster for fields applied along certain directions. At high fields, the distribution is much hotter and the holes are scattered randomly throughout the Brillouin zone by the deformation-potential scattering. Therefore the majority of ionizing holes start from anywhere within the Brillouin zone, and the directional dependence of the rate vanishes.

The hole impact-ionization rate is much lower in InP than in GaAs, as seen from a comparison of Figs. 13 and 14. The Monte Carlo calculations, presented in Fig. 14 are made using a universal impact-ionization threshold of 1.55 eV and a universal  $p$  factor of 20.0. Since the impact-ionization rate is low in InP, far fewer ionization events occur in it than in GaAs. There is a much greater statistical uncertainty in the impact-ionization calculations in InP than in GaAs. This may explain the greater deviation between the experimental InP data and the calculated data at low fields.

For the cases discussed above, where the ionization threshold and  $p$  factor are the same for each band, the majority of ionizing holes originate within the heavy-hole band. Through the applied fields of interest here, the relative percentage of impact-ionizing holes in the various bands remains roughly constant in GaAs. The heavy holes contribute the most to the ionization rate, for the above parameter set and the split-off holes contribute the least. This is true in both GaAs and InP, but the split-off holes in GaAs are more important to the overall impact-ionization rate since the split-off energy is less in GaAs than in InP.

The hole impact-ionization rate is much lower in InP

than in GaAs, although the relative strength of impact ionization, treated as a scattering mechanism, is greater in InP than in GaAs. This apparent paradox can be explained by comparing the scattering rates and density of states between the two materials. The total phonon scattering rate in InP is significantly larger than the total phonon scattering rate in GaAs, as seen from a comparison of Figs. 9 and 10. Competing phonon scattering processes reduce the probability of impact ionization. Consequently, since the phonon scattering rate is much higher in InP than in GaAs, the probability of impact ionization in InP is greatly reduced.

The difference in the scattering rates between GaAs and InP is due to the different density of states in each material (Fig. 15). The density of states is significantly higher in InP at energies above 1.0 eV. When the density of states increases, it becomes more difficult for a hole to drift to states at and above threshold. Hence fewer holes in InP will reach sufficiently high energies for impact ionization to occur.

Recent experimental measurements of the hole impact-ionization rate in Al-Ga-Sb alloys suggest that the impact ionization is strongly influenced by holes in the split-off band.<sup>41,42</sup> Hildebrand *et al.*<sup>41,42</sup> have suggested that a “resonance” occurs in the impact-ionization rate when the split-off energy is equal to the energy-band gap. Although no “resonance,” as defined by Hildebrand,<sup>41</sup> can occur in either GaAs or InP, since the energy gap is much larger than the split-off energy, it appears likely, based on these results, that the split-off band can be the dominant factor in hole impact ionization, contrary to the previously presented results. We have found an additional set of parameters for GaAs, in which the split-off holes are the dominant impact-ionizing carriers. In this case, the threshold for impact ionization in the split-off band is equal to the band-gap energy, while the ionization threshold is significantly higher in both the heavy- and light-hole bands. The  $p$  value remains the same as before in GaAs, namely, 0.25, for all three bands.  $E_{th}$  for the heavy and light holes is then 1.80 eV. The hole impact-ionization rate using these parameters is presented for GaAs in Fig. 16. Again, the calculations fit the experimental data well through a wide range of applied electric fields. This model of impact ionization due to the split-off holes may be more appropriate than the heavy-hole ionization model on the basis of the Anderson-Crowell criterium,<sup>38</sup> which favors the values of  $E_{th}$  obtained for the split-off model.

The difference between the hole impact-ionization rates in GaAs and InP in this case is easily explained. The split-off energy is larger in InP than in GaAs. The density of states in the split-off band then, is smaller in InP than in GaAs at or near the ionization threshold energy. Consequently, transfer of holes to the split-off band in InP is more unlikely than in GaAs at an energy near the impact-ionization threshold energy. Results from the Monte Carlo simulation indicate that the experimental data in InP cannot be fit by assuming that the impact ionization is due largely to the split-off holes. From this result it appears that the split-off band does not effect the impact-ionization rate significantly unless the split-off en-



ergy is small with respect to the band-gap energy, or the split-off energy is exactly equal to the band-gap energy such that a "resonance" in the impact-ionization rate can occur. Notice, however, that this conclusion rests entirely on the calculated, high phonon scattering rate. According to our experience with other materials, the high  $p$  factor and low threshold (which are necessary to fit the experimental data) suggest that the phonon scattering rate may be slightly overestimated.

Therefore, based upon the above Monte Carlo calculations it cannot be uniquely determined which physical picture is correct in GaAs; the hole impact-ionization rate is dominated by the split-off band or the heavy-hole band. A work is planned to investigate the nature of the "resonance" effect in  $\text{Ga}_{1-x}\text{Al}_x\text{Sb}$  which may further determine the importance of the split-off band in hole impact ionization.

In a previous work<sup>23</sup> we have determined, by again using the Monte Carlo technique, the *electron* impact-ionization rate in both GaAs and InP. The results of these calculations are presented along with the experimental measurements<sup>19,20</sup> in Figs. 17 and 18. Comparison of these curves with Figs. 13 and 14 indicates that  $\alpha$  is greater than  $\beta$  in GaAs, while  $\beta$  is greater than  $\alpha$  in InP.

The Monte Carlo calculations of the electron impact-ionization rate determines the ionization threshold in GaAs to be 1.70 eV and the  $p$  factor to be 0.5.<sup>23</sup> In InP the ionization threshold is found to be 2.10 eV, while the corresponding  $p$  factor is 0.5.<sup>23</sup> Comparing the results of the calculated electron and hole impact-ionization rates, which are fit to the existing experimental measurements, reveals that the ionization threshold energy is the same for both electrons and holes in GaAs, namely 1.70 eV, while the  $p$  factors differ by a factor of 2. The ionization threshold energy for hole impact ionization, 1.55 eV, is much smaller than the threshold for electron ionization, 2.10 eV, in InP.

The density of states in the valence band is much flatter than the density of states in the conduction band in either GaAs or InP, as seen from a comparison of Figs. 15 and 19. Therefore it is easier for an electron to drift to higher energies than a hole even though the phonon scattering rates are comparable. Consequently, one expects the electron impact-ionization rate to be greater than the hole ion-

ization rate if the threshold energies are the same. This is the case in GaAs, and the electron impact-ionization rate is stronger than the hole ionization rate. However, in InP the hole threshold appears much smaller than the electron threshold. The difference in the thresholds is then sufficiently large that it is easier for the holes to impact-ionize. Consequently,  $\beta$  is greater than  $\alpha$  in InP.

## VI. CONCLUSIONS

We have calculated, via a Monte Carlo approach, the impact-ionization rate and steady-state drift velocities of holes in GaAs and InP. Two models of hole impact ionization have been presented. The first model assumes a universal threshold energy for the heavy-hole, light-hole, and split-off bands. This model predicts that the heavy holes are the dominant ionizing agents. The second model assumes a much smaller threshold in the split-off band which results in the split-off holes dominating the impact-ionization process. A small anisotropy in the impact-ionization rate is observed at low fields, while no anisotropy occurs using either model at high fields.

Previously calculated results of the electron impact-ionization rate in GaAs and InP are compared with the hole ionization rate presented here. The comparison shows that the electron impact-ionization rate is greater than the hole impact-ionization rate in GaAs, while in InP the hole ionization rate is larger than the electron ionization rate, in accordance with recent experimental measurements. The reversal in the ratio of  $\alpha$  and  $\beta$  appears to be due to the difference between the density of states of the conduction band and that of the valence band, as well as the different electron and hole ionization threshold energies.

## ACKNOWLEDGMENTS

We would like to thank Dr. J. Y. Tang for many helpful discussions on hole transport. We are also grateful to Dr. Y. C. Chang for his help in calculating the band structure using the  $\vec{k} \cdot \vec{p}$  method. Special thanks go to Dr. F. Capasso for pointing out inconsistencies in the original manuscript. The technical assistance of J. T. Gladdin and R. F. MacFarlane is also greatly appreciated. This work was sponsored by the U. S. Office of Naval Research and the U. S. Joint Services Electronics Program.

<sup>1</sup>S. M. Sze, *Physics of Semiconducting Devices*, 2nd ed. (Wiley, New York, 1981).

<sup>2</sup>P. Chatterjee, presented at the Third Workshop on the Physics of Submicron Structures, University of Illinois, Urbana, Illinois, 1982 (unpublished).

<sup>3</sup>*Physics of Nonlinear Transport in Semiconductors*, edited by D. K. Ferry, J. R. Barker, and C. Jacoboni (Plenum, New York, 1980).

<sup>4</sup>H. L. Grubin, D. K. Ferry, G. J. Iafrate, and J. R. Barker, in *VLSI Electronics: Microstructure Science*, edited by N. G. Einspruch (Academic, New York, 1981).

<sup>5</sup>G. E. Stillman and C. M. Wolfe, in *Semiconductors and Semimetals*, edited by R. K. Willardson and A. C. Beer (Academic, New York, 1977), Vol. 12, pp. 291–393.

<sup>6</sup>R. J. McIntyre, *IEEE Trans. Electron. Dev.* **ED-13**, 164 (1966).

<sup>7</sup>G. E. Bulman, Ph.D. thesis, University of Illinois, 1983.

<sup>8</sup>R. Chin, N. Holonyak, Jr., G. E. Stillman, J. Y. Tang, and K. Hess, *Electron Lett.* **16**, 467 (1980).

<sup>9</sup>F. Capasso, *IEEE Trans. Electron. Dev.* **ED-29**, 1388 (1982).

<sup>10</sup>F. Capasso, W. T. Tsang, A. L. Hutchinson, and G. F. Williams, *Appl. Phys. Lett.* **40**, 38 (1982).

<sup>11</sup>P. A. Wolff, *Phys. Rev.* **95**, 1415 (1954).

<sup>12</sup>W. Shockley, *Solid-State Electron.* **2**, 35 (1961).

<sup>13</sup>G. A. Baraff, *Phys. Rev.* **128**, 2507 (1962).

<sup>14</sup>L. V. Keldysh, *Zh. Eksp. Teor. Fiz.* **48**, 1692 (1965) [*Sov. Phys.—JETP* **21**, 1135 (1965)].

<sup>15</sup>W. P. Dumke, *Phys. Rev.* **167**, 783 (1968).

<sup>16</sup>H. Shichijo and K. Hess, *Phys. Rev. B* **23**, 4197 (1981).

<sup>17</sup>B. K. Ridley, *J. Phys. C* **16**, 4733 (1983).

<sup>18</sup>B. K. Ridley, *J. Phys. C* **16**, 3378 (1983).

<sup>19</sup>G. E. Bulman, V. M. Robbins, K. F. Brennan, K. Hess, and

- G. E. Stillman, *IEEE Electron Device Lett.* **EDL-4**, 181 (1983).
- <sup>20</sup>L. W. Cook, G. E. Bulman, and G. E. Stillman, *Appl. Phys. Lett.* **40**, 589 (1982).
- <sup>21</sup>N. Tabatabaie, V. M. Robbins, K. F. Brennan, K. Hess, and G. E. Stillman, in *Proceeding of the 41st Annual Device Research Conference*, Burlington, Vermont, 1983 (unpublished).
- <sup>22</sup>E. O. Kane, *J. Phys. Chem. Solids* **1**, 633 (1980).
- <sup>23</sup>K. Brennan and K. Hess (unpublished).
- <sup>24</sup>M. L. Cohen and T. K. Bergstresser, *Phys. Rev.* **141**, 789 (1966).
- <sup>25</sup>J. D. Wiley, in *Semiconductors and Semimetals*, edited by R. K. Willardson and A. C. Beer (Academic, New York, 1975), Vol. 10, pp. 91–174.
- <sup>26</sup>M. Costato and L. Reggiani, *Phys. Status Solidi B* **58**, 471 (1973).
- <sup>27</sup>M. Costato and L. Reggiani, *Phys. Status Solidi B* **58**, 47 (1973).
- <sup>28</sup>Y. C. Chang, D. Z.-Y. Ting, J. Y. Tang, and K. Hess, *Appl. Phys. Lett.* **42**, 76 (1983).
- <sup>29</sup>J. Y. Tang, Ph.D. thesis, University of Illinois, 1983.
- <sup>30</sup>C. Canali, C. Jacoboni, F. Nava, G. Ottaviani, and A. Albeirgi-Quaranta, *Phys. Rev. B* **12**, 2265 (1975).
- <sup>31</sup>G. L. Bir and G. E. Pikus, *Fiz. Tverd. Tela (Lenin)* **3**, 2287 (1961) [*Sov. Phys.—Solid State* **2**, 2039 (1961)].
- <sup>32</sup>J. D. Wiley, *Solid State Commun.* **8**, 1865 (1970).
- <sup>33</sup>J. Y. Tang and K. Hess, *Appl. Phys.* **54**, 5139 (1983).
- <sup>34</sup>L. H. Holway, S. R. Steele, and M. G. Alderstein, in *Proceedings of the Seventh Biennial Cornell Electrical Engineering Conference* (Cornell University Press, Ithaca, N.Y., 1979), pp. 199–208.
- <sup>35</sup>T. H. Windhorn, T. J. Roth, L. M. Zinkiewicz, O. L. Gaddy, and G. E. Stillman, *Appl. Phys. Lett.* **40**, 513 (1982).
- <sup>36</sup>T. H. Windhorn, L. W. Cook, M. A. Haase, and G. E. Stillman (unpublished).
- <sup>37</sup>P. A. Houston and A. G. R. Evans, *Solid-State Electron.* **20**, 197 (1977).
- <sup>38</sup>C. L. Anderson and C. R. Crowell, *Phys. Rev. B* **5**, 2267 (1972).
- <sup>39</sup>E. O. Kane, *Phys. Rev.* **159**, 624 (1967).
- <sup>40</sup>T. P. Pearsall, R. E. Nahory, and J. R. Chelikowsky, in *Proceedings of the Sixth International Symposium on GaAs and Related Compounds, St. Louis, 1976*, edited by Lester F. Eastman (IOP, Bristol, 1977), Chap. 6, pp. 331–338.
- <sup>41</sup>O. Hildebrand, W. Kuebart, K. W. Benz, and M. H. Pilkuhn, *IEEE J. Quantum Electron.* **QE-17**, 284 (1981).
- <sup>42</sup>O. Hildebrand, W. Kuebart, and M. H. Pilkuhn, *Appl. Phys. Lett.* **37**, 801 (1980).
- <sup>43</sup>M. Neuberger, *Handbook of Electronic Materials* (Plenum, New York, 1971), Vol. 2, pp. 45–56.
- <sup>44</sup>M. Neuberger, *Handbook of Electronic Materials*, Ref. 43, pp. 108–112.
- <sup>45</sup>T. P. Pearsall, F. Capasso, R. E. Nahory, M. A. Pollak, and J. R. Chelikowsky, *Solid State Electron.* **21**, 297 (1978).